Calibrated Hot Box Tests of Thermal Performance of Concrete Walls

M.G. Van Geem A.E. Fiorato D.W. Musser

ABSTRACT: The object of research described in this paper was to evaluate and compare thermal performance of selected concrete walls. Walls were subjected to steady-state, transient, and periodically varying temperature conditions in a calibrated hot box. Steady-state tests were used to define heat transmission coefficients. Data obtained during periodic temperature variations were used to define dynamic thermal response of the walls.

Normal-weight, structural lightweight, and low density concretes were tested. These concretes had unit weights ranging from approximately 50 to 145 pcf. Thermal conductivity of the concretes, derived from calibrated hot box tests, ranged from approximately 1.5 to 12.0 Btu·in./hr·ft²·°F. Conductivities derived from calibrated hot box tests were compared with results from guarded hot plate and hot wire tests. Hot wire tests were also used to evaluate the influence of moisture on thermal conductivity. Data obtained from dynamic tests were compared with steady-state calculations. In addition, data were compared with calculations of dynamic response made using measured values of thermal properties.

INTRODUCTION

Tests were conducted to evaluate thermal performance of solid concrete walls under steady-state and dynamic temperature conditions. Dynamic tests provided a measure of thermal response under selected temperature ranges. A simulated sol-air dynamic cycle was selected to permit comparison of results with those obtained in previous investigations.[1,2,3]

Objectives of the experimental investigation were to evaluate and compare thermal performance of three concrete walls. Wall C1 was constructed of normal-weight concrete, wall C2 of structural lightweight concrete, and wall C3 of low density concrete. This paper summarizes experimental results for the three walls. Detailed results for each wall are covered in separate reports.[4,5,6]

Also included in this paper are data on thermal conductivity of control specimens cast from the same concrete used in the walls.

Walls were tested in the calibrated hot box facility of Portland Cement Association's Construction Technology Laboratories (CTL).

TEST SPECIMENS

The test walls had overall nominal dimensions of 103 x 103 in. (2.62 x 2.62 m). All wall construction, including concrete mixing and casting, was performed at CTL.

M. G. Van Geem, Research Engineer, Construction Methods Department, A. E. Fiorato, Director, Concrete Materials Research Department, and D. W. Musser, Director, Construction Methods Department, Construction Technology Laboratories, a Division of the Portland Cement Association, 5420 Old Orchard Road, Skokie, Illinois 60077.

Construction

The test walls were all constructed of reinforced concrete. They differed, however, in the type of concrete and size of reinforcement. Mix designs of the walls are given in Tab. 1. Details of wall construction are given in individual wall reports.[7,8,9]

Wall C1 was a normal-weight concrete wall having an average measured thickness of 8.31 in. (211 mm). Elgin coarse and fine aggregates were used in the concrete. Nominal maximum size of the coarse gravel was 3/4 in. (19 mm). Elgin aggregates are dolomitic.[10]

Wall C2 was a structural lightweight concrete wall with an average thickness of 8.28 in. (210 mm). Expanded shale aggregate with a nominal maximum size of 3/4 in. (19 mm) was used.

Wall C3 was a low density concrete wall with an average thickness of 8.52 in. (216 mm). Expanded perlite aggregate was used in the concrete; its maximum size was No. 8 (2.36 mm) mesh. Expanded perlite is produced by heating and, thereby, expanding perlite, a volcanic glass.

Reinforcement in walls C1 and C2 consisted of a single layer of No. 5 bars spaced 12-in. (305 mm) center to center in each direction as shown in Fig. 1. A single mesh of 6-mm diameter deformed bar reinforcement was used in wall C3. Walls were cast horizontally.

Reinforcing bars were supported at a height of 4 in. (102 mm) off the formwork base by concrete chairs. Chair supports were constructed using the same concrete used for the wall. Concrete rather than steel or plastic chairs were used since precise measurement of wall thermal properties required the elimination of possible thermal bridges.

Walls C1 and C2 were allowed to cure in formwork for 7 days. Wall C3 was cured in formwork for 14 days. After removing formwork, the walls were allowed to air cure in the laboratory at an air temperature of 73±5°F (23±3°C) and 45±15% RH. Walls C1 and C2 were air cured for 5 months before testing. Wall C3 was air cured for 6 months.

Wall faces were coated with a cementitious waterproofing material that seals minor surface imperfections. A textured, white acrylic paint was used as a finish coat. These coatings provided a uniform surface for both wall faces. Wall edges were left uncoated.

Unit Weight

Weights of walls C1, C2, and C3, and corresponding 6 x 12-in. (152 x 305-mm) control specimens were determined periodically while air drying. The volume of each wall was determined from average measured dimensions. Volume of each cylinder was calculated from cylinder weights in air and immersed in water. Unit weights were then calculated from measured weights and volumes.

Unit weights for walls C1, C2, and C3 and the 6 x 12-in. (152 x 305-mm) cylinders are illustrated in Fig. 2. Unit weights decreased with time for the first two to three months and then remained fairly constant. The reduction in unit weight is due to evaporation of free water from concrete. Wall unit weights at the time of calibrated hot box tests were determined to be 144 pcf (2300 kg/m^3) for wall C1, 102 pcf (1630 kg/m^3) for wall C2, and 46 pcf (740 kg/m^3) for wall C3.

Moisture Content

Average moisture content of each wall at the time of calibrated hot box tests was determined from air-dry unit weight of the wall and average oven-dry unit weight of selected control specimens. Average moisture contents relative to oven-dry weight at the time of test were 2.1% for wall C1, 8.5% for wall C2, and 9.5% for wall C3.

CALIBRATED HOT BOX TEST FACILITY

Tests were conducted in the calibrated hot box facility shown in Fig. 3. This facility was developed to permit realistic evaluation of thermal performance of large wall assemblies under steady-state or dynamic temperature conditions. Tests were performed in accordance with ASTM:C976, Test Method for Thermal Performance of Building Assemblies by Means of a Calibrated Hot Box.[11]

Description

The following is a brief description of the calibrated hot box (details are available in Ref. 12). The facility consists of two highly insulated chambers, as shown in Fig. 4. Walls, ceiling, and floors of each chamber are insulated with foamed urethane sheets to obtain a final thickness of 12 in. (305 mm). During tests, the chambers are clamped tightly against an insulating frame that surrounds the test wall. Air in each chamber is conditioned by heating and cooling equipment to obtain desired temperatures on each side of the test wall.

The outdoor chamber can be held at a constant temperature or cycled between -15 and 130°F (-26 and 54°C). Temperature cycles can be programmed to obtain the desired time-temperature relationship. The indoor chamber, which simulates an indoor environment, can be maintained at a constant room temperature between 65 and 80°F (18 and 27°C).

The facility was designed to accommodate walls with thermal resistance values ranging from 1.5 to 20 $hr \cdot ft^2 \cdot °F/Btu$ (0.26 to 3.52 $K \cdot m^2/W$).

Instrumentation

Instrumentation was designed to monitor temperatures inside and outside of the chambers, air and surface temperatures on both sides of the test wall, interior temperatures within the test wall, laboratory air temperature, and heating energy input to the indoor chamber. Supplementary measurements monitor indoor cooling system performance as well as heat flux at selected locations on the specimen and chamber surfaces. Basically, the instrumentation provides a means of monitoring the energy required to maintain constant temperature in the indoor chamber while temperatures in the outdoor chamber are varied. This energy, when corrected for thermal losses, provides a measure of heat flow through the test wall.

Calibration Procedure

The following is a brief description of the calibration procedure used for determining heat flow through the test wall. Details are available in Ref. 13.

Heat flow is determined from measurements of the amount of energy input to the indoor chamber to maintain a constant temperature. The measured energy input must be adjusted for heat losses. Figure 5 shows sources of heat losses and gains by the indoor chamber

where

Q_w = heat transfer through test wall, Btu/hr (W·hr/hr)
Q_c = heat removed by indoor chamber cooling, Btu/hr (W·hr/hr)
Q_h = heat supplied by indoor electrical resistance heaters, Btu/hr (W·hr/hr)
Q_{fan} = heat supplied by indoor circulation fan, Btu/hr (W·hr/hr)
Q_ℓ = heat loss/gain from laboratory, Btu/hr (W·hr/hr)
Q_f = heat loss/gain from flanking path around specimen, Btu/hr (W·hr/hr)

Since net energy into the control volume equals zero, heat transfer through the test wall can be expressed by the following energy balance equation

$$Q_w = Q_c - Q_h - Q_{fan} - Q_\ell - Q_f \quad (1)$$

A watt-hour transducer is used to measure Q_h and Q_{fan}. The value of Q_ℓ is calculated from measured temperatures. Heat flux transducers are used to check calculations. Steady-state calibrated hot box tests of two "standard" calibration specimens were used to refine calculations of Q_ℓ and Q_c and to determine Q_f. In addition to flanking losses, other miscellaneous losses from the indoor chamber are included in Q_f.[14]

For steady-state and dynamic tests performed on the concrete walls, the indoor-chamber air and laboratory air temperatures were maintained at the same nominal value, 72°F (22°C), to minimize laboratory losses. Thus, the value of Q_ℓ is small relative to other terms of the energy balance equation.

STEADY-STATE THERMAL PROPERTIES OF THE CONCRETES

Thermal conductivity of the concrete walls was derived from steady-state tests using the calibrated hot box. The guarded hot plate (ASTM:C177) and hot wire methods were also used to determine thermal conductivity of wall concrete. Values of thermal transmittance, specific

heat, and thermal diffusivity are not presented in this paper but are discussed in reports for each individual wall.[15,16,17]

Guarded Hot Plate

For each wall, average apparent thermal conductivity of two 5.6 x 5.6 x 1.95-in. (142 x 142 x 49.5-mm) samples was determined[18] in accordance with ASTM:C177, Standard Test Method for Steady-State Thermal Transmission Properties by Means of the Guarded Hot Plate.[19] Specimens were cured for 7 days in molds and approximately one year at 73±5°F (23±3°C) and 45± 15% RH. Samples were cut to size from 16 x 16 x 2-in. (406 x 406 x 51-mm) specimens and were oven dried before testing.

Common practice in hot plate tests is for thermocouples to be placed in surface contact with the test sample. However, for tests conducted on these concrete specimens thermocouples were embedded into surfaces of each concrete specimen. Fine wire thermocouples in silica protective tubes were fitted tightly into 0.020 x 0.020-in. (0.51 x 0.51-mm) grooves that had been cut into the surfaces. According to Tye and Spinney[20] if thermocouples are not embedded in the specimen, a contact resistance can be introduced between the thermocouple junction and the concrete surface and will result in an artificially large temperature difference across the specimen. Consequently, the derived value of conductivity will be too low.

Apparent thermal conductivities of oven-dried samples obtained by hot plate tests at a mean specimen temperature of 70°F (21°C) were 16.1 Btu·in./hr·ft^2·°F (2.32 W/m·K) for wall C1, 4.49 Btu·in./hr·ft^2·°F (0.647 W/m·K) for wall C2, and 1.44 Btu·in./hr·ft^2·°F (0.208 W/m·K) for wall C3.

Hot Wire Method

The hot wire method[21] was also used to determine apparent thermal conductivity of air-dry and oven-dry prisms. For these tests, concrete prisms were cast with a nickel-chromium constantan thermocouple embedded along their central longitudinal axis.

To test a specimen using the hot wire method, a thermocouple reading is taken, electrical current is supplied to the wire, and additional temperature readings are made at selected intervals for a period of 10 minutes. Apparent thermal conductivity is calculated from the measured current, the resistance of the wire, and the thermocouple readings.

Thermal conductivity of each type of concrete was measured on two sets of specimens. A first set of three specimens was cured in molds for 7 days and then air cured at 73±5°F (23±3°C) and 45±15% RH. Conductivity of these specimens was determined for the air-dry and oven-dry conditions. Average apparent thermal conductivities are given in Tab. 2.

A second set of specimens was cured in molds for 24 hours and then moist cured at 73±3°F (23±1.7°C) and 100% RH for a minimum of 3 months. Tests were performed on three specimens for walls C1 and C3 and one specimen for wall C2. Specimens were first tested immediately after removal from the moist cure room. Tests were then conducted after specimens had been air dried for 7, 26, and 54 days. A final test was performed on specimens after they had been oven-dried. Hot wire test results for the moist-cured samples are shown in Tab. 3.

Calibrated Hot Box

Apparent thermal conductivity of the concrete walls was also derived from steady-state calibrated hot box tests. Steady-state tests are conducted by maintaining constant indoor and outdoor chamber temperatures. Conductivity values were calculated from data collected when specimen temperatures reached equilibrium and the rate of heat flow through the test wall was constant.

Apparent thermal conductivity was determined from the following relationship

$$k = \frac{3.413\ t \cdot Q_w}{A \cdot (t_2 - t_1)} \qquad (2)$$

where

k = thermal conductivity, Btu·in./hr·ft^2·°F

t = wall thickness, in.
Q_w = heat transfer through test wall, W·hr/hr
A_w = area of wall surface normal to heat flow, ft^2
t_2 = average temperature of outside wall surface, °F
t_1 = average temperature of inside wall surface, °F
3.413 = conversion factor from W·hr/hr to Btu/hr

The amount of heat passing through the test wall, Q_w, was calculated from Eq 1.

Values of conductivity are reported in Tab. 4 for selected mean wall temperatures tested. Mean wall temperature is the average of the indoor wall surface temperature, t_1, and the outdoor wall surface temperature, t_2.

Discussion of Results

Figure 6 shows the ratio of conductivity of concrete at a particular moisture content to conductivity of the oven-dry concrete plotted as a function of moisture content. Data were obtained from hot wire tests listed in Table 3. Increased moisture content of the concrete increased conductivity.

Thermal conductivity versus moisture content relationships proposed in Refs. 22, 23, and 24 are also shown in Fig. 6. Hot wire test data for walls C1 and C3 lie between the curve proposed in Ref. 23 and the line proposed in Ref. 24. Wall C2 concrete generally shows a smaller increase in conductivity with moisture content than is predicted by any of the proposed relationships.

Unit weight of concrete strongly influences thermal conductivity. Figure 7 illustrates that values of thermal conductivity for oven-dry concretes range from approximately 1.0 Btu·in./hr·ft^2·°F (0.14 W/m·K) for wall C3 to 16 Btu·in./hr·ft^2·°F (2.3 W/m·K) for wall C1.

Figure 7 also shows that measured values of thermal conductivity varied with the test method used. Guarded hot plate and hot wire test results are for air-cured oven-dry samples. Calibrated hot box results were derived from thermal conductivity values of the walls at a mean temperature of 70°F (21°C), converted to oven-dry values. Values were calculated assuming a 6% increase in thermal conductivity for each 1% increase in moisture content, by weight, relative to oven-dry density.[25]

Thermal conductivity of oven-dry concrete has been estimated from[26]

$$\begin{aligned} \text{IP units:} \quad & k = 0.5e^{0.02\rho} \\ \text{SI units:} \quad & k = 0.072e^{1250\rho} \end{aligned} \tag{3}$$

where

k = thermal conductivity, Btu·in./hr·ft^2·°F (W/m·K)
ρ = oven-dry unit weight of concrete, pcf (kg/cm^3)
e = base of the system of natural logarithms

Estimated values of thermal conductivity calculated from Eq 3 are also plotted in Fig. 7.

Figure 7 shows that conductivities of oven-dry normal-weight concrete determined using the guarded hot plate and hot wire methods are substantially greater than estimated values. Results from calibrated hot box tests are closer to the values estimated from Eq 3.

Results from hot wire and guarded hot plate tests are higher than those from calibrated hot box tests. This difference is attributed to contact-resistance-temperature measurement error. A surface-contact thermal resistance results from any thin air gap between the thermocouple wire and the concrete at their point of contact. This additional thermal resistance can occur when thermocouples are not embedded in the test material. For materials with high thermal conductivities, the surface-contact resistance can be a significant part of the total measured resistance.[27] Surface-contact thermal resistance may be of the same order of magnitude as the resistance of the normal-weight concrete wall.

For calibrated hot box tests, thermocouple wires were applied to the walls in accordance with ASTM:C976, Section 5.7.1, which states that requirements of the standard are presumed to be met if wire is "taped, cemented or otherwise held in thermal contact with the surface using materials of emittance close to that of the surface."

Apparent thermal conductivity results for normal-weight and structural lightweight concrete walls tested in the calibrated hot box were lower than results determined using the guarded hot plate, with thermocouples placed in grooves, or the hot wire method, with embedded thermocouples. These results are indicative of the influence of contact resistance on determination of apparent thermal conductivity for walls C1 and C2. This influence is negligible for wall C3.

As can be seen in Tab. 4, results from calibrated hot box tests indicated an increase in thermal conductivity of concrete with temperature.

DYNAMIC CALIBRATED HOT BOX TESTS

Although steady-state tests provide a measure of resistance to heat flow, response of walls to temperature changes is a function of both thermal resistance and heat storage capacity. Dynamic tests are a means of evaluating thermal response under controlled conditions that simulate temperature changes actually encountered in building envelopes. These tests provide a comparative measure of response and also can be used to verify analytical models for transient heat flow.

Test Procedure

Dynamic tests were conducted by maintaining calibrated hot box indoor air temperatures constant while outdoor air temperatures were cycled over a predetermined time-versus-temperature relationship. Energy required to maintain a constant indoor air temperature was monitored as a function of time. The rate of heat flow through the test wall was determined using Eq 1 for hourly averages of data.

Three 24-hr (diurnal) temperature cycles were used in this investigation. The first cycle applied to each wall was based on a simulated sol-air* cycle used by the National Bureau of Standards in evaluating dynamic thermal performance of an experimental masonry building.[28] It represents a large variation in outdoor temperature over a 24-hr period. The mean outdoor temperature of the cycle was approximately equal to the mean indoor temperature. This cycle, denoted NBS, was run to permit comparison of results with those from earlier tests.[29,30,31]

Two additional sol-air temperature cycles were run. The NBS+10 cycle was derived by increasing hourly outdoor temperatures of the NBS cycle by 10°F (6°C). The NBS-10 cycle was derived by decreasing hourly outdoor temperatures by 10°F (6°C).

For all tests, dynamic cycles were repeated until conditions of equilibrium were obtained. Equilibrium conditions were evaluated by consistency of applied temperatures and measured energy response. Each test required approximately four to six days for completion. After equilibrium conditions were reached, the test was continued for three days. Results are based on average readings for at least three consecutive 24-hr cycles.

Dynamic Test Results

Results for the NBS-10 cycle are given in Figs. 8 through 10. Results from the other two dynamic cycles are presented in Refs. 32, 33, and 34.

Figures 8 (a), 9 (a), and 10 (a) give measured air, surface, and internal wall temperatures for the three walls. The following notation is used to designate average measured temperatures:

t_i = indoor chamber air temperature, °F (°C)
t_1 = wall surface temperature, indoor side, °F (°C)
t_3 = internal wall temperature at approximate midthickness, °F (°C)
t_2 = wall surface temperature, outdoor side, °F (°C)
t_o = outdoor chamber air temperature, °F (°C)

*Sol-air temperature is that temperature of outdoor air that, in the absence of all radiation exchanges, would give the same rate of heat entry into the surface as would exist with the actual combination of incident solar radiation, radiant energy exchange, and convective heat exchange with outdoor air.[31]

Figures 8 (b), 9 (b), and 10 (b) present measured heat flow rates, Q_w, through the walls calculated from Eq 1. Heat flow rates measured by a heat flow meter on the inside surface of the test wall, Q_{hfm}, and those predicted by steady-state analysis, Q_{ss}, are also shown. Positive values represent heat flow from the outdoor to the indoor side of the wall. All data are averages from three consecutive 24-hr cycles.

Heat flow meter data were calibrated using results of steady-state calibrated hot box tests. Heat flow meter readings were plotted against measured heat flow rates, Q_w, for the steady-state tests. A linear regression analysis of the data was used to obtain a calibration factor for the heat flow meter.

Heat flow rates predicted by steady-state analysis were calculated on an hourly basis from wall surface temperatures using

$$Q_{ss} = \frac{A \cdot C \cdot (t_2 - t_1)}{3.413} \qquad (4)$$

where

Q_{ss} = heat transfer through test wall, W·hr/hr
A = area of wall surface normal to heat flow, ft^2
C = average thermal conductance, Btu/hr·ft^2·°F
t_2 = average temperature of outside wall surface, °F
t_1 = average temperature of inside wall surface, °F
3.413 = conversion factor from W·hr/hr to Btu/hr

Values of thermal conductance were determined from calibrated hot box test data.

Peaks in the measured heat flow curve, Q_w, have smaller amplitudes and occur later than those on the Q_{ss} curve.

Thermal Lag. Thermal lag is a measure of the response of inside and outside surface temperatures and heat flow to fluctuations in outdoor temperature. Lag is indicative of both thermal resistance and heat storage capacity of the test specimen.

Thermal lag is quantified by two measures in Tab. 5. In one measure, lag was calculated as the time required for the maximum or minimum indoor surface temperature to be reached after the maximum or minimum outdoor air temperature was attained. In the second measure, lag was calculated as the time required for the maximum or minimum heat flow rate, Q_w, to be reached after the maximum or minimum heat flow rate based on steady-state predictions, Q_{ss}, was attained. This is illustrated in Fig. 8 (b).

The two measures of lag give the same results for walls C1 and C2. For wall C3 the average difference between the two measures is approximately one hour. Maximums and minimums for wall C3 are less prominent than those for walls C1 and C2. Therefore, determination of the exact location of peaks is subject to more variability for wall C3 than for walls C1 and C2.

Heat flow meter data, denoted by Q_{hfm} in the figures, consistently show the same lag time as measured heat flow data, Q_w.

The low density concrete, wall C3, has the greatest lag time. This result is consistent with that indicated by thermo-physical properties of the concretes.

Thermal lag increases with an increase in[35]

$$M = \sqrt{\frac{L^2/\alpha}{P}} \qquad (5)$$

where

L = wall thickness, ft (m)
P = length of dynamic cycle, hr
α = thermal diffusivity, ft^2/hr (m^2/s)

$$\alpha = \frac{k}{\rho \cdot c} \qquad (6)$$

where

k = thermal conductivity, Btu/hr·ft·°F (W/m·K)
ρ = unit weight, pcf (kg/m^3)
c = specific heat, Btu/lb·°F (J/kg·K)

Wall thickness, length of dynamic cycle, and specific heat are approximately equal for walls C1, C2, and C3. Therefore, differences in thermal lag for the three walls are due to differences in thermal conductivity and unit weight.

Values of M for walls C2 and C3 are, respectively, 1.3 and 1.7 times greater than the value of M for wall C1. Thermal lags for walls C2 and C3 are, respectively, 1.4 and 2.1 times greater than the thermal lag for wall C1. Thus, the measured increase in thermal lag is consistent with that indicated by theory.

Thermal lag is of interest because the time of occurrence of peak heat flows will affect the overall response of the building envelope. If the envelope can be effectively used to delay the occurrence of peak loads, it may be possible to improve overall energy efficiency. The lag effect is also of interest in passive solar applications.

Reduction in Amplitude. Reduction in amplitude, or damping, of heat flows is influenced by the same factors that affect thermal lag. Both thermal resistance and heat storage capacity affect damping. Reduction in amplitude is illustrated in Fig. 8 (b).

Values of percent reduction in amplitude listed in Tab. 5 were calculated by

$$A = \left[1 - \frac{Q'_w - \bar{Q}_w}{Q'_{ss} - \bar{Q}_w} \right] \cdot 100 \qquad (7)$$

where

A = percent reduction in amplitude
$\bar{Q}_w$ = mean measured heat flow through wall
Q'_w = maximum or minimum measured heat flow through wall
Q'_{ss} = maximum or minimum heat flow through wall, predicted by steady-state analysis

Reduction in amplitude also increases as M increases.[36] Reductions in amplitude (percent) for walls C2 and C3 are 1.2 and 1.4 times greater than that for wall C1. This compares to values of M for walls C2 and C3 that are, respectively, 1.33 and 1.67 times greater than the value of M for wall C1.

Maximum heat flow through a wall is important in determining the peak energy load for a building. If peak heat flows are reduced, peak energy demands will decrease. Storage capacity, as well as thermal transmittance of each wall in a building envelope, influences peak energy requirements.

Amplitudes for heat flow meter data, Q_{hfm}, are less than amplitudes for measured heat flow, Q_w. This occurs for all walls and can be seen in Figs. 8, 9, and 10. Amplitudes for Q_{hfm} and Q_w differ because of the physical effect of a heat flow meter mounted on a wall. Heat flow paths are altered at the location of the heat flow meter. Calibration of the heat flow meter using steady-state results does not correct for dynamic effects at the meter location.

Measured Energy. Results of dynamic tests were also compared using measures of energy expended in maintaining a constant indoor temperature while outdoor temperatures were varied. Energy expended is a measure of heat flow through the test wall. It should be noted that comparison of measured energy values for the test walls is limited to specimens and dynamic cycles evaluated in this program. Results are for diurnal test cycles and should not be arbitrarily assumed to represent annual heating and cooling loads. In addition, results are for individual opaque wall assemblies. As such, they are representative of only one component of the building envelope.

The curves marked "Q_w" in Figs. 8 (b), 9 (b), and 10 (b) were used to determine total energy expended. For each dynamic test, the sum of the absolute values of positive and negative areas between the Q_w curve and the zero heat flow rate line was calculated to obtain total energy over a 24-hr period. This value is denoted as Q'_a in Tab. 5.

A similar procedure was used to calculate total energy based on steady-state predictions over a 24-hr period. This value, Q'_b in Tab. 5, is the sum of the absolute values of positive and negative areas under the steady-state curves, Q_{ss}.

Values of Q'_a, Q'_b, and Q'_a/Q'_b for the NBS-10 test cycle are listed in Tab. 5 for each wall. For all three walls, total measured energy, Q'_a, was considerably less than total energy based based on steady-state predictions, Q'_b.

Thermal conductivity and unit weight influence total measured energy. If total measured energy were dependent solely on thermal conductivity, the ratio of total energy for two walls would be equal to the ratio of conductivities of the walls. Conductivities for walls C1 and C2 are, respectively, 8.4 and 3.4 times greater than the conductivity of wall C3. Values of total energy for walls C1 and C2 are, respectively, 5.1 and 2.8 times greater than that for wall C3. Therefore, total measured energy is less than what would be predicted on the basis of conductivity of wall concrete.

These results confirm data obtained in earlier investigations that indicate that thermal mass has a beneficial effect for diurnal cycles in which outdoor temperatures fluctuate above and below indoor temperatures to cause reversals of heat flow.

Measured net energy for dynamic tests theoretically should be equal to net energy based on steady-state predictions. Measured net energy for a 24-hr periodic cycle is equal to the difference between positive and negative areas under the heat flow-rate curves. Steady-state net energy was calculated according to the following equation:

$$Q_n = \frac{C \cdot A \cdot (t_1^m - t_2^m) \cdot 24}{3.413} \qquad (8)$$

where

Q_n = net energy based on steady-state predictions
C = average measured thermal conductance, Btu/hr·ft^2·°F
A = area of wall surface normal to heat flow, ft^2
t_1^m = mean temperature of inside wall surface over 24-hr cycle, °F
t_2^m = mean temperature of outside wall surface over 24-hr cycle, °F
3.413 = conversion factor from W·hr/hr to Btu/hr

A comparison of calculated and measured net energy data is given in Tab. 5. Measured and calculated values agree to within 8%, indicating that measured data are reasonable.

SUMMARY AND CONCLUSIONS

This report presents results of an experimental investigation of heat transmission characteristics of a normal-weight structural concrete wall, a structural lightweight concrete wall, and a low density concrete wall under steady-state and dynamic temperature conditions. Companion concrete control specimens were also tested to determine physical and thermal properties.

The following conclusions are based on results obtained in this investigation.

1. Unit weights of walls C1, C2, and C3 were 144, 102, and 46 pcf (2300, 1630, and 740 kg/m^3), respectively.

2. Moisture contents, expressed as percent relative to oven-dry weight, for walls C1, C2, and C3 were 2.1, 8.5, and 9.5, respectively.

3. Apparent thermal conductivities derived from steady-state calibrated hot box tests for walls C1, C2, and C3 were 11.7, 4.7, and 1.4 Btu·in./hr·ft^2·°F (1.69, 0.68, and 0.20 W/m·K), respectively.

4. Apparent thermal conductivities of oven-dry concrete obtained from guarded hot plate tests with embedded thermocouples were 16.1, 4.49, and 1.44 Btu·in./hr·ft^2·°F (2.32, 0.647, and 0.208 W/m·K) for walls C1, C2, and C3, respectively.

5. Measured conductivities of air-dry concrete determined from hot wire tests were 20.3, 6.03, and 3.05 Btu·in./hr·ft^2·°F (2.93, 0.870, and 0.440 W/m·K) for walls C1, C2, and C3, respectively.

6. Thermal conductivity of concrete increases with density.

7. Values of apparent thermal conductivity vary with test method. Differences are most significant for normal-weight and structural lightweight concrete.

8. An increase in moisture content of concrete increases thermal conductivity.

9. Heat storage capacity of the concrete walls delayed heat flow through the specimen (as indicated by thermal lag). Average thermal lags of walls C1, C2, and C3 were 4, 5.5, and 8.5 hours, respectively.

10. Heat storage capacity of the concrete walls reduced peak heat flows through the specimen (as indicated by the damping effect). Average reductions in amplitude of heat flow for walls C1, C2, and C3 were 45, 54, and 63%, respectively.

11. Energy requirements for a 24-hr period were lowest for the low density concrete wall. Total energy expended depends on concrete thermal conductivity and unit weight.

Results described in this report provide data on thermal response of three concrete walls subjected to steady-state and dynamic temperature cycles. A complete analysis of building energy requirements must include consideration of the entire building envelope, the building orientation and operation, and yearly weather conditions. Data developed in this experimental program provide a quantitative basis for modeling the building envelope, which is part of the overall energy analysis process.

REFERENCES

1. A.E. Fiorato, and E. Bravinsky, Heat Transfer Characteristics of Walls Under Arizona Temperature Conditions (Skokie, IL: Construction Technology Laboratories, Portland Cement Association, 1981).

2. A.E. Fiorato, and C.R. Cruz, Thermal Performance of Masonry Walls, Research and Development Bulletin RD071 (Skokie, IL: Portland Cement Association, 1980).

3. A.E. Fiorato, Heat Transfer Characteristics of Walls Under Dynamic Temperature Conditions, Research and Development Bulletin RD075 (Skokie, IL: Portland Cement Association, 1981).

4. M.G. Van Geem, A.E. Fiorato, and J.T. Julien, Heat Transfer Characteristics of a Normal-Weight Concrete Wall (Skokie, IL: Construction Technology Laboratories, Portland Cement Association, 1983).

5. M.G. Van Geem, and A.E. Fiorato, Heat Transfer Characteristics of a Structural Lightweight Concrete Wall (to be published, Skokie, IL: Construction Technology Laboratories, Portland Cement Association).

6. M.G. Van Geem and A.E. Fiorato, Heat Transfer Characteristics of a Low Density Concrete Wall (to be published, Skokie, IL: Construction Technology Laboratories, Portland Cement Association).

7. Van Geem, Heat Transfer Characteristics of a Normal-Weight Concrete Wall, pp. 2-8.

8. Van Geem, Heat Transfer Characteristics of a Structural Lightweight Concrete Wall.

9. Van Geem, Heat Transfer Characteristics of a Low Density Concrete Wall.

10. M.S. Abrams, Compressive Strength of Concrete at Temperatures to 1600 F, Research and Development Bulletin RD016 (Skokie, IL: Portland Cement Association, 1973) p. 1.

11. 1983 Annual Book of ASTM Standards (Philadelphia, PA: American Society for Testing and Materials, 1983).

12. A.E. Fiorato, "Laboratory Tests of Thermal Performance of Exterior Walls," Proceedings of the ASHRAE/DOE-ORNL Conference on Thermal Performance of the Exterior Envelopes of Buildings (Orlando, FL: ASHRAE SP28, 1979) pp. 221-236.

13. M.G. Van Geem, A.E. Fiorato, and D.W. Musser, Calibration and Test Procedures for the Calibrated Hot Box Method of Evaluating Thermal Performance (to be published, Skokie, IL: Construction Technology Laboratories, Portland Cement Association).

14. Van Geem, Heat Transfer Characteristics of a Normal-Weight Concrete Wall, pp. 30-31.

15. Van Geem, Heat Transfer Characteristics of a Normal-Weight Concrete Wall, pp. 31-33, 47-50.

16. Van Geem, Heat Transfer Characteristics of a Structural Lightweight Concrete Wall.

17. Van Geem, Heat Transfer Characteristics of a Low Density Concrete Wall.

18. Andre Desjarlais, The Thermal Conductivity and Thermal Resistance of Three Specimens of Concrete Materials, Dynatech Report No. PCA-1 (Cambridge, MA: Dynatech R/D Co., 1982).

19. 1981 Annual Book of ASTM Standards, Part 18 (Philadelphia, PA: American Society for Testing and Materials, 1981), pp. 20-53.

20. R.P. Tye, and S.C. Spinney, "Thermal Conductivity of Concrete: Measurement Problems and Effect of Moisture" (Paper presented at Meeting of Commission of BI of Institute International Du Froid, Washington, D. C., September 14-15, 1976), p. 3.

21. A.E. Lentz, and G.E. Monfore, Thermal Conductivity of Concrete at Very Low Temperatures," Journal of the PCA Research and Development Laboratories, 7:2 (May 1965), pp. 39-46.

22. Harold W. Brewer, "General Relation of Heat Flow Factors to the Unit Weight of Concrete," Journal of the PCA Research and Development Laboratories, 9:1 (January 1967), pp. 48-60.

23. Max Jakob, Heat Transfer, Volume I (New York: John Wiley & Sons, Inc., 1949), pp. 93-94.

24. M.G. Van Geem and A.E. Fiorato, Thermal Properties of Masonry Materials for Passive Solar Design - A State-of-the-Art Review (Skokie, IL: Construction Technology Laboratories, Portland Cement Association, 1983) pp. 46-48.

25. Rudolph V.C. Valore, Jr., "Calculation of U-Values of Hollow Concrete Masonry," Concrete International, 2:2 (Feb. 1980) pp. 40-63.

26. Valore, "Calculation of U-Values of Hollow Concrete Masonry," pp. 41-47.

27. Tye, "Thermal Conductivity of Concrete: Measurement Problems and Effect of Moisture," p.3.

28. B.A. Peavy, F.J. Powell, and D.M. Burch, Dynamic Thermal Performance of an Experimental Masonry Building, Building Science Series 45 (Washington DC: U.S. Department of Commerce, National Bureau of Standards, 1973).

29 Fiorato, Heat Transfer Characteristics of Walls Under Arizona Temperature Conditions, pp. 30-54.

30. Fiorato, Thermal Performance of Masonry Walls, pp. 7-9, 11-17.

31. Fiorato, Heat Transfer Characteristics of Walls Under Dynamic Temperature Conditions, pp. 5-16.

32. Van Geem, Heat Transfer Characteristics of a Normal-Weight Concrete Wall, pp. 54-76.

33. Van Geem, Heat Transfer Characteristics of a Structural Lightweight Concrete Wall.

34. Van Geem, Heat Transfer Characteristics of a Low Density Concrete Wall.

35. Ken Childs, Thermal Mass Assessment, Part of the National Program for Building Thermal Envelope Systems and Insulating Materials (to be published, Oak Ridge, TN: Oak Ridge National Laboratory).

36. Childs, Thermal Mass Assessment.

ACKNOWLEDGMENTS

This paper was prepared as part of a project sponsored jointly by the U.S. Department of Energy, Division of Buildings and Community Systems, and the Portland Cement Association. The work is under subcontract ORNL/SUB42539/1 with Oak Ridge National Laboratory (ORNL). It is part of the National Program Plan for Building Thermal Envelope Systems and Insulating Materials.

The work was performed in the Engineering Development Division of the Construction Technology Laboratories, a Division of the Portland Cement Association, under the direction of Dr. W. G. Corley, Divisional Director.

Construction of the lightweight structural concrete wall was sponsored by the Solite Corp., West New York, NJ. Expanded shale aggregate used in the mix was provided by Solite.

Construction of the low density concrete wall was sponsored by the Perlite Institute, Inc., New York. Expanded perlite aggregate and mix preparation for wall C3 were provided by Silbrico Corp. G. Wavering of Silbrico Corp. provided advice and assistance on wall construction.

Exterior coating materials for the three walls were provided by Thoro System Products. Advice and assistance on application of the coatings were provided by W. Downs and S. Downs of Thoro System Products, Buffalo Grove, IL.

Construction and preparation of specimens were performed by E. A. Valko, J. A. Chavez, and P. P. Hordorwich. J. A. Chavez also assisted with data reduction.

E. Ringquist provided editorial assistance in preparation of the manuscript. The manuscript was typed by personnel of the Portland Cement Association's Word Processing Department. R. Reichenbach drafted the figures.

Any opinions, findings, and conclusions expressed in this paper are those of the authors and do not necessarily reflect the views of the United States Government or any agency thereof.

TABLE 1

Concrete Mix Characteristics*

Wall	Mix Proportions, lb/yd^3 (kg/m^3)				Vinsol Resin,*** ml/lb cement	Fresh Concrete			
	Cement	Fine Aggregate (SSD)**	Coarse Aggregate (SSD)	Water		W/C	Unit Wt., pcf$_3$ (kg/m^3)	Air Content, %	Slump in. (mm)
C1	463 (275)	1472 (873)	1746 (1036)	280 (166)	1.50	0.60	146.8 (2352)	5.9	2.9 (74)
C2	519 (308)	1150 (682)	780 (463)	340 (202)	1.75	0.66	103.1 (1652)	6.3	2.8 (71)
C3	721 (428)	248**** (147)	0	538 (319)	4.72	0.75	56.1 (899)	-	-

*Values given are average of 10 batches for walls C1 and C2, and three batches for wall C3.
**Saturated surface dry (SSD).
***Air entraining agent.
****Dry weight of perlite.

TABLE 2

Apparent Thermal Conductivity of Air-Cured Specimens, Hot Wire Method

Wall	Air Dry				Oven Dry	
	Age at Time of Test, days	Density, pcf (kg/m^3)	Moisture Content, % by oven-dry wt.	Thermal Conductivity, Btu·in./hr·ft^2·°F (W/m·K)	Density, pcf (kg/m^3)	Thermal Conductivity, Btu·in./hr·ft^2·°F (W/m·K)
C1	154	143 (2290)	1.8	20.3 (2.93)	140 (2240)	13.6 (1.96)
C2	98	99 (1580)	5.2	6.0 (0.87)	94 (1500)	4.2 (0.61)
C3	78	56 (900)	17.3	3.1 (0.44)	48 (770)	1.5 (0.22)

TABLE 3

Apparent Thermal Conductivity of Concretes
At Different Moisture Contents, Hot Wire Method

Wall	Length of Time Air Cured, days	Moisture Content, % oven-dry weight	Unit Weight, pcf (kg/m^3)	Moisture Content, % volume	k Thermal Conductivity, $\frac{Btu \cdot in.}{hr \cdot ft^2 \cdot °F}$ (W/m·K)	$\frac{k_{(moist)}}{k_{(ovendry)}}$
C1*	64+	0	141 (2260)	0	14.0 (2.02)	1
	54	3.1	145 (2320)	6.9	21.3 (3.07)	1.52
	26	3.8	146 (2340)	8.5	23.7 (3.42)	1.69
	7	4.4	147 (2350)	9.9	21.5 (3.10)	1.54
	0	5.3	148 (2370)	11.9	25.7 (3.71)	1.84
C2**	63+	0	93 (1490)	0	5.14 (0.740)	1.00
	54	9.5	102 (1630)	14.1	6.85 (0.987)	1.33
	26	10.5	103 (1650)	15.7	7.02 (1.012)	1.37
	7	11.6	104 (1660)	17.3	6.98 (1.007)	1.36
	0	13.6	106 (1700)	20.2	9.91 (1.429)	1.93
C3***	63+	0	46 (740)	0	1.32 (0.190)	1
	54	28.9	59 (940)	21.2	3.12 (0.450)	2.36
	26	34.6	62 (990)	25.4	3.18 (0.459)	2.41
	7	40.8	64 (1020)	29.9	3.20 (0.461)	2.42
	0	48.7	68 (1090)	35.7	3.91 (0.564)	2.96

*All specimens cured 24 hours in molds and 174 days at 73±3°F (23±1.7°C) and 100% RH prior to air curing.
**All specimens cured 24 hours in molds and 119 days at 73±3°F (23±1.7°C) and 100% RH prior to air curing.
***All specimens cured 24 hours in molds and 100 days at 73±3°F (23±1.7°C) and 100% RH prior to air curing.
+Ovendry

TABLE 4

Apparent Thermal Conductivity Derived From
Calibrated Hot Box Steady-State Test Results

Wall	Mean Wall Temperature, °F (°C)	Thermal Conductivity, $\frac{Btu \cdot in.}{hr \cdot ft^2 \cdot °F}$ (W/m·K)
C1	37.0 (2.8)	11.63 (1.68)
	54.9 (12.7)	11.64 (1.65)
	101.0 (38.3)	11.79 (1.70)
C2	33.9 (1.1)	4.66 (0.672)
	51.9 (11.1)	4.69 (0.676)
	87.7 (30.9)	4.77 (0.688)
	99.0 (37.2)	4.83 (0.696)
C3	52.6 (11.4)	1.38 (0.199)
	89.5 (31.9)	1.50 (0.216)
	99.8 (37.7)	1.56 (0.225)

TABLE 5

Summary of Dynamic Test Results For NBS-10 Test Cycle

Wall	Thermal Lag, hr					Reduction in Amplitude, percent			Total Energy, W·hr/hr			Net Energy, W·hr/hr		
	t_o vs t_1		Q_{ss} vs Q_w		Avg.									
	@ Max	@ Min	@ Max	@ Min		@ Max	@ Min	Avg.	Q'_a	Q'_b	Q'_a/Q'_b	Measured	Calculated	Meas./Calc.
Wall C1	4.5	3	4.5	3	4	50	40	45	4636	7074	0.66	-4342	-4330	1.00
Wall C2	6	5	6	5	5.5	57	50	54	2554	4282	0.60	-2510	-2636	0.95
Wall C3	8.5	7	9	9	8.5	67	58	63	909	1717	0.53	-909	-989	0.92

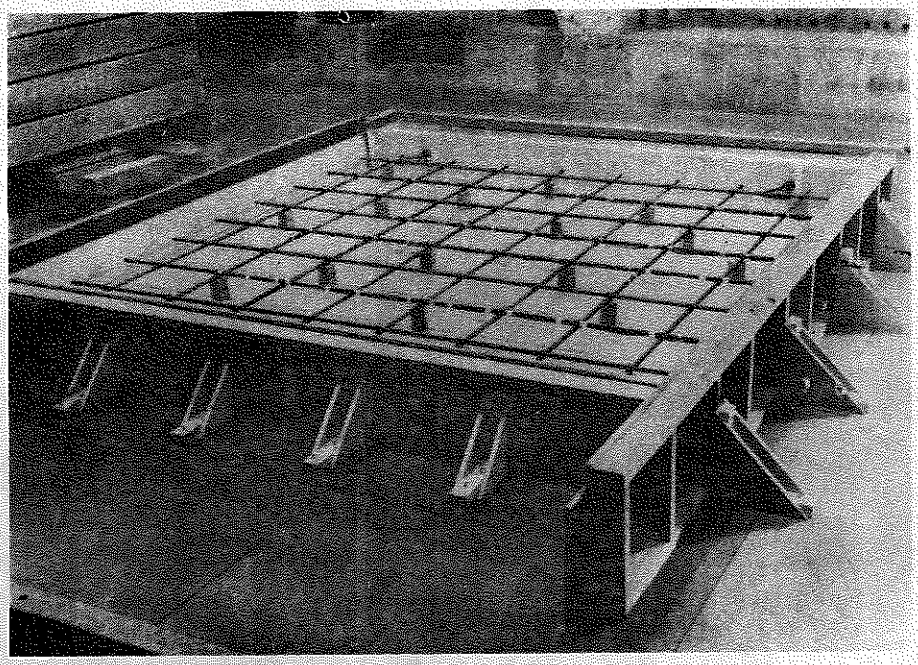

Figure 1. Formwork and reinforcement for concrete walls

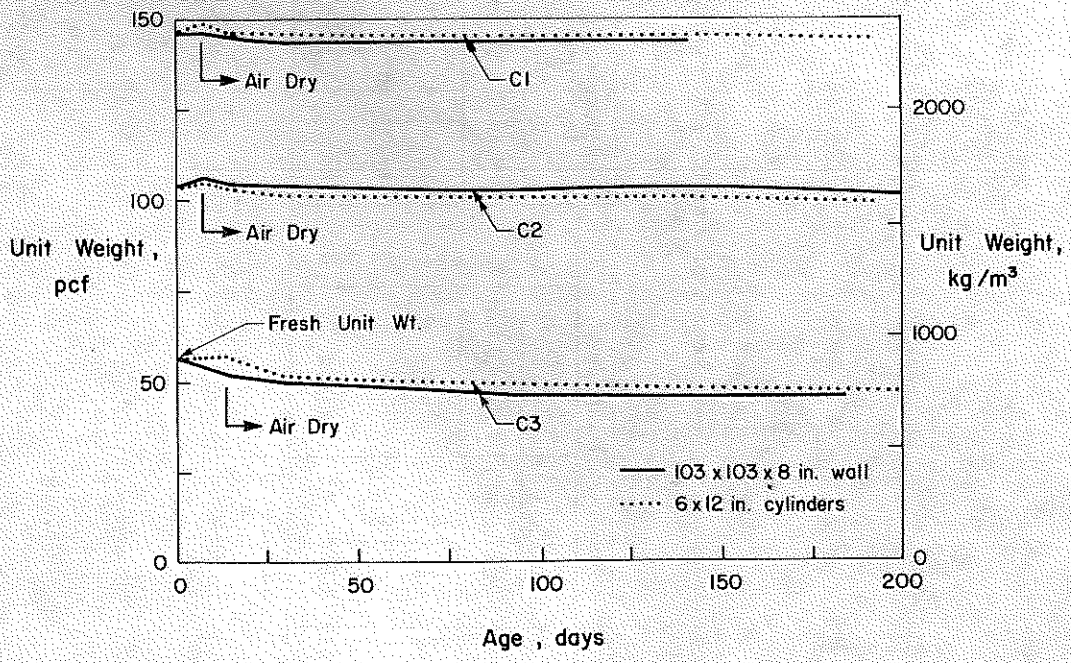

Figure 2. Unit weights of walls and control cylinders

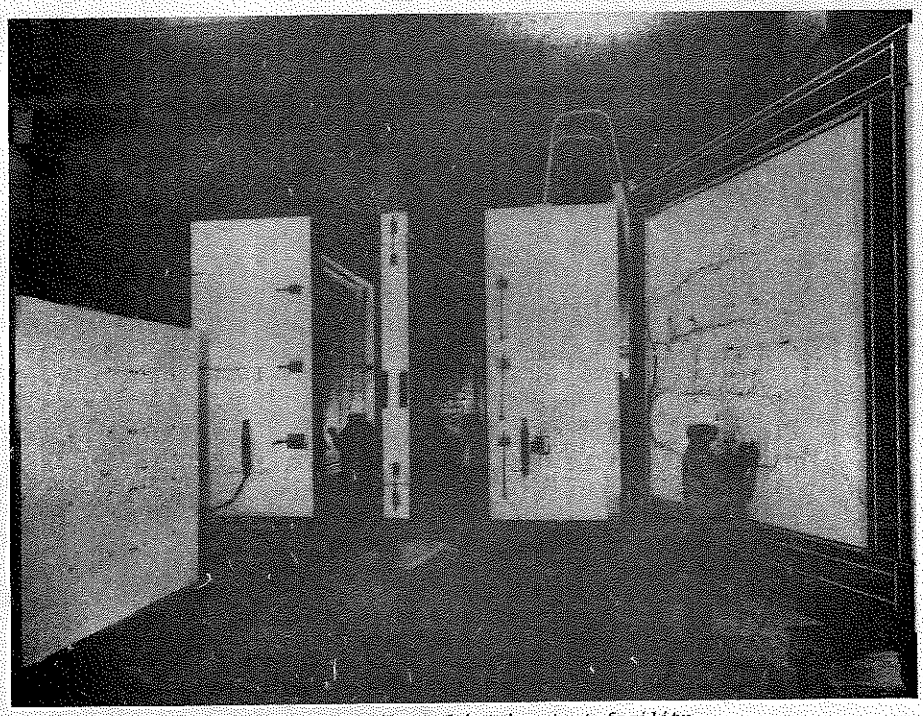

Figure 3. Calibrated hot box test facility

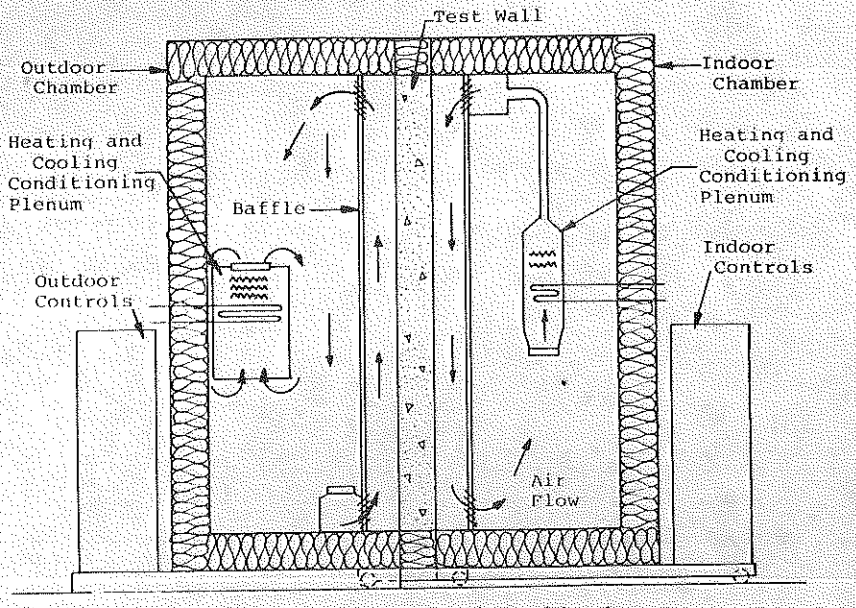

Figure 4. Schematic of calibrated hot box

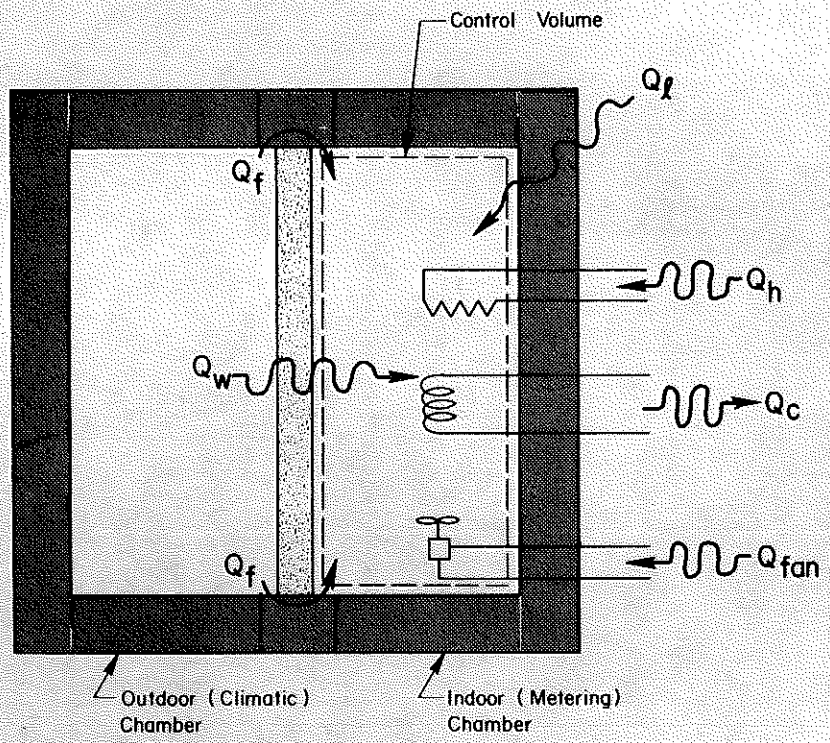

Figure 5. Indoor (metering) chamber energy balance

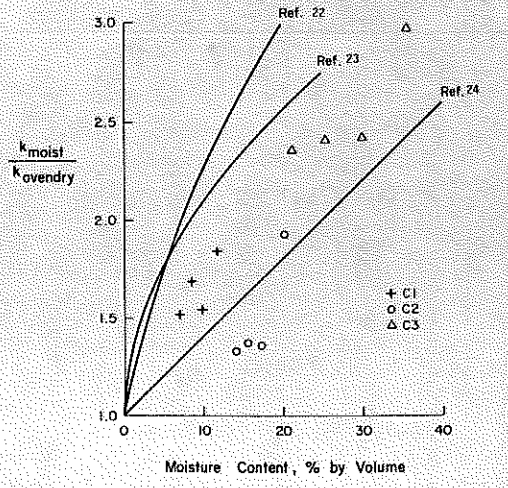

Figure 6. Thermal conductivity of concrete as a function of moisture content

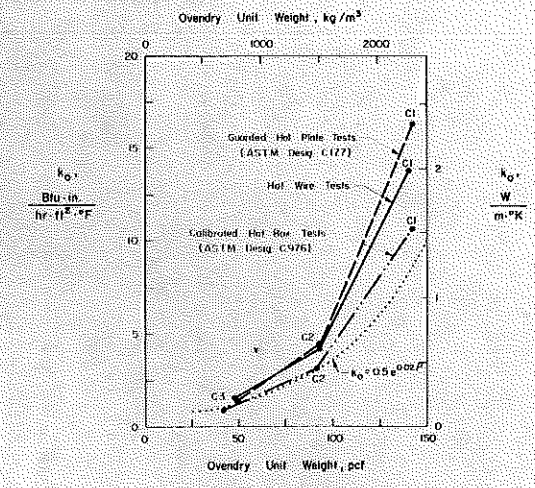

Figure 7. Thermal conductivity of concrete as a function of unit weight

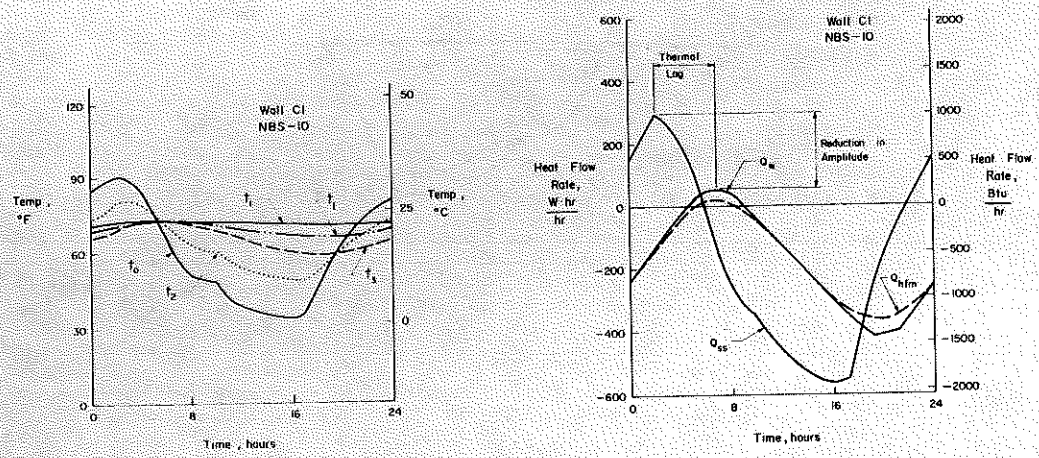

(a) measured temperatures

(b) measured heat flow

Figure 8. Dynamic test results of wall C1 for NBS-10 test cycle

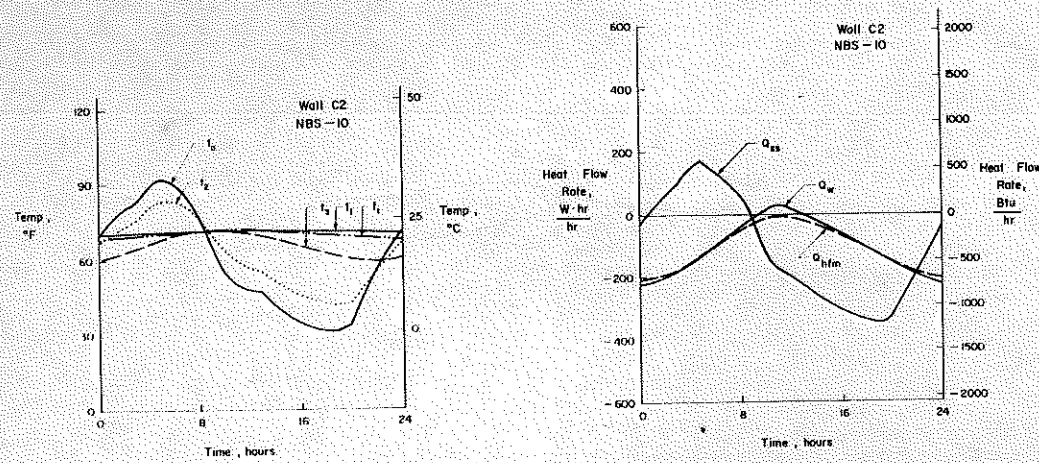

(a) measured temperatures

(b) measured heat flow

Figure 9. Dymanic test results of wall C2 for NBS-10 test cycle

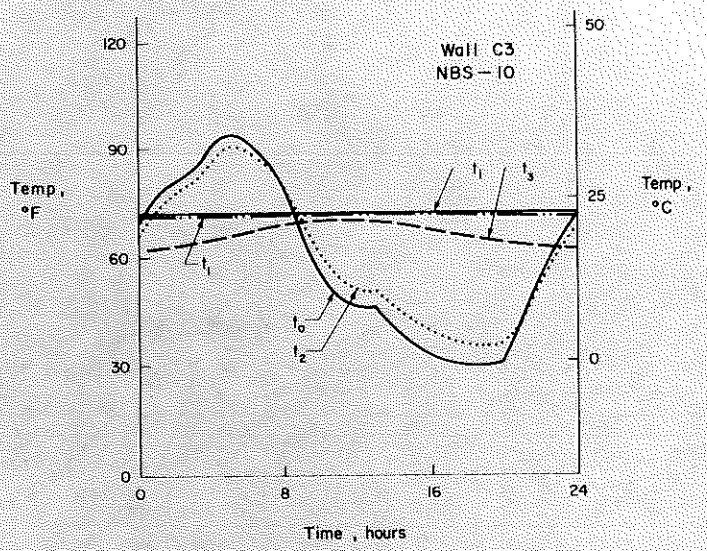

(a) measured temperatures

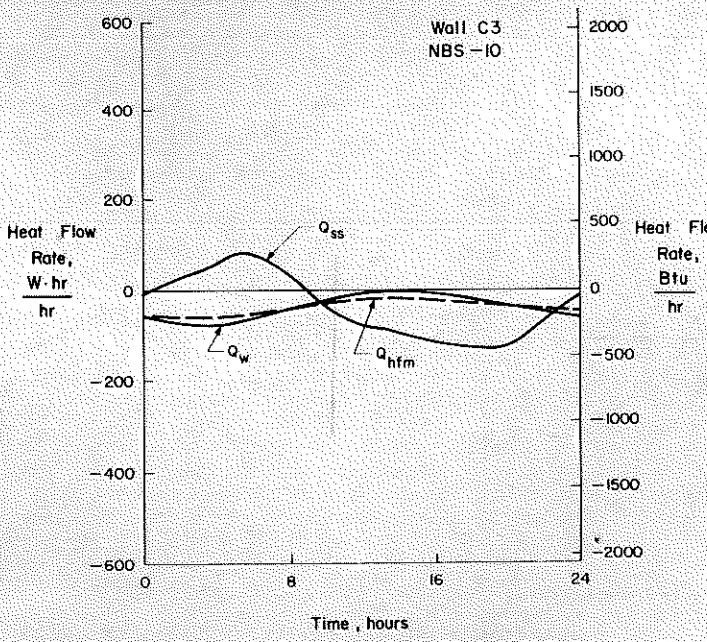

(b) measured heat flow

Figure 10. Dynamic test results of wall C3 for NBS-10 test cycle

Discussion

R.J. Berg, Architect, Veterans Administration, Washington, DC: Publish results for walls measured to show temperature outside--30°F to 40°F versus inside temperature +75°F. Do you get any appreciable effect to show temperature outside +80°F to +110°F. How much dynamic effect occurs under these two conditions for time lag? Time lag appears to be significant where heat and cooling loads occur alternately within a short period of time, but not for great extremes of temperatures where either heating or cooling load would not alternate, i.e., midwinter and midsummer.

A. E. Fiorato: Values of time lag were essentially constant for all temperature cycles applied to each wall. Temperature cycles that caused heat flow in only one direction gave the same time lag as those that caused reversals of heat flow through the wall. Time lag is dependent on thermophysical properties of the wall material.

S. Jurovics, IBM, Los Angeles, CA: Did you do any comparison of your measurements with the response factor method, rather than steady-state method? Did you compare your time lag with classical theory, e.g., Carslow and Jaegar?

A.E. Fiorato: This paper compares dynamic test results with theory presented in the draft report entitled "Thermal Mass Assessment" by K. W. Childs of Oak Ridge National Laboratory (ORNL). Dynamic test data are currently being compared to analytical results using the response factor method. This comparison is part of a joint project with ORNL.

R.P. Bowent, Resch. Officer, Building Resch., NCR Canada, Ottawa, Ontatio: How were flanking losses established? Were temperatures near the perimeter monitored?

A.E. Fiorato: Flanking losses were determined from steady-state calibrated hot box tests of standard calibration walls with known R Values. Measured values of heat flow through the wall were corrected for losses and compared to theoretical values. Flanking loss was taken as the difference between measured and theoretical values of heat flow. This "flanking loss" term thus includes other miscellaneous losses from the indoor chamber. A more detailed explanation is presented in the report for the normal-weight concrete wall:

> Van Geem M. G., Fiorato, A. E., and Julien, J. T., "Heat Transfer Characteristics of a Normal-Weight Concrete Wall," Construction Technology Laboratores, Portland Cememt Association, Skokie, 1983, 89 pages.

P.R. Achenbach, Conslt., McLean, VA: Presumably you inserted the various wall specimens into the test frame. How much clearance was required and how did you seal the joint between the wall and the frame?

A.E. Fiorato: The insultating frame is made up of our pieces that clamp together around the test wall. Interior faces in contact with the test specimen are covered with 1/4-in. polyurethane foam material. Nominal test wall dimensions are 103x103-in. Dimensions of the concrete walls ranged from 102-15/16-in. to 103-3/16-in.

After each test specimen was mounted in the frame, joints between the wall and frame were caulked and taped.

S.L. Matthews, Vice-Pres., Tech. Systems, Rockwool Industries, Inc., Denver, CO: Have you run

a test without the flywheel effect, that is, where outdoor temperature is never as low or as high as indoor?

You can then say that without flywheel there is no lag value or energy savings. Therefore, it does not work without flywheel.

A.E. Fiorato: Time lag remains essentially constant for different temperature cycles applied to a wall. All temperature cycles will result in the same time lag regardless of whether or not the outdoor chamber temperature fluctuates above and below the indoor chamber temperatures. Time lag is dependent on the material properties.

Dynamic tests of massive walls indicated significant reductions in total heat flow when outdoor chamber temperatures fluctuated above and below indoor chamber temperatures to cause reversal of heat flow through the test wall. These reductions relate to energy required to maintain indoor chamber temperatures constant when compared to steady-state energy predictions.

For test in which temperature cycles were such that heat flow reversal did not occur, total heat flow was proportional to wall U-value.